Deformation Mechanisms of Polypropylene/Polystyrene Multilayered Films

S. Scholtyssek,[1] F. Pfeifer,[2] V. Seydewitz,[1] R. Adhikari,[3] H. W. Siesler,[2] G. H. Michler[1]

[1]*Institute of Physics, Martin Luther University Halle, Wittenberg D 06099, Halle (Saale), Germany*
[2]*Department of Physical Chemistry, University of Duisburg-Essen, Essen D 45117, Germany*
[3]*Central Department of Chemistry, Tribhuvan University, P. O. Box 24411, Kathmandu, Nepal*

Received 30 May 2011; accepted 12 December 2011
DOI 10.1002/app.36657
Published online in Wiley Online Library (wileyonlinelibrary.com).

ABSTRACT: Multilayered composites of polypropylene (PP) and polystyrene (PS) fabricated by a layer-multiplying coextrusion technique are described. The aim of this investigation was to find a correlation between the morphology and the mechanical and micromechanical deformation behavior. The multilayered films had primarily continuous layers, exhibiting only few defects in layer construction and turning into an irregularly layered system when the calculated layer thickness was only 5 nm. The morphology and layer thickness of both the PP and PS layers affected the mechanical and the micromechanical behavior, which was brittle for the films having PS layers thicker than 75 nm and ductile when the PS layers were 50 nm and thinner. Transmission electron microscopy showed crazes in the thicker PS layers and homogeneous deformation in the thinner ones. The molecular orientation during deformation of the ductile films was calculated from rheo-optical measurements with Fourier transform infrared spectroscopy. © 2012 Wiley Periodicals, Inc. J Appl Polym Sci 000: 000–000, 2012

Key words: FT-IR; mechanical properties; nanolayers; TEM

INTRODUCTION

Microstructured and nanostructured materials with specific mechanical and other functional properties have been the focus of much current research activity. The aim is to produce materials that adopt the good properties of combined single materials or, in the ideal case, that even have superior properties. Different strategies have been used to produce such materials. One is the multilayer coextrusion technique, which is used to fabricate films with tens to thousands of alternating ultrathin polymer layers.[1] To understand the size-scale-dependent properties is a precondition as bulk polymers become thinner and thinner. Polymer characteristics that can be adapted to specific applications are the permeability,[2,3] optical properties,[4] and electrical properties.[5]

In ref. [6], a summary of the processing and application of multilayer coextrusion is given. Most of the studies on multilayered films have reported combinations of two amorphous polymers. Composites of poly(styrene–acrylonitrile) and polycarbonate (PC),[7–9] PC and poly(methyl methacrylate),[10,11] and polystyrene (PS) and poly(methyl methacrylate)[12] are very well known. Multilayered films having at least one crystalline polymer are less investigated because of their complicated processing. However, as shown in literature and previous investigations, it is possible to combine semicrystalline and amorphous polymers, such as polypropylene (PP) and PS, by a multilayer coextrusion process, which creates ultrathin layers down to 10 nm in size.[13,14] Other combinations with at least one crystalline polymer have been described, too.[15–18]

When adapting special characteristics, as described previously, the mechanical properties of the system are affected. Micromechanical deformation behavior has been examined on poly(styrene–acrylonitrile)/PC[9] and polyethylene terephthalate (PET)/PC[19] systems, among others. In addition to the dependence on the volume fraction of the single polymers, an essential influence of layer thickness on the stress–strain behavior was found in both systems.

The goal of this study was to find relationships between the morphology, micromechanical deformation behavior, and molecular deformation in multilayered composites of the model PP/PS system.

EXPERIMENTAL

Materials and sample preparation

In this study, multilayered composite films of 1024 alternating layers of PP and PS were produced at

Correspondence to: S. Scholtyssek (stefanie.scholtyssek@physik.uni-halle.de).

Contract grant sponsors: German Research Foundation (DFG), Max-Buchner-Forschungsstiftung (for financial support and a research scholarship to S.S.).

TABLE I
Characteristics of the Investigated Multilayered PP/PS Samples

PP/PS	Film thickness (μm)	Number of layers	PP calculated single-layer thickness (nm)	PS calculated single-layer thickness (nm)
90/10	250	1024	450	50
90/10	125	1024	225	25
90/10	25	1024	45	5
70/30	250	1024	350	150
70/30	125	1024	175	75
70/30	25	1024	35	15

Case Western Reserve University (Cleveland, OH) by E. Baer and A. Hiltner with the well-established multilayer coextrusion procedure [1]. The films had compositions of 90/10 and 70/30 PP/PS and three different film thicknesses, 250, 125, and 25 nm. From these processing parameters, the thickness of a single layer could be calculated to be between 35 and 450 μm for PP and between 5 and 150 nm for PS. An overview of the samples investigated in this work and the calculated single-layer thicknesses are given in Table I.

Microscopic techniques

The morphology of the samples was investigated with a transmission electron microscope (LEO 912, Zeiss, Oberkochen, Germany) operated at an accelerating voltage of 120 kV. Therefore, properly prepared cross sections of the films were stained with ruthenium tetroxide (RuO_4) vapor for several hours at 60°C. Then, ultrathin sections (80 nm thick) were prepared by an ultramicrotome (Ultracut E, Leica, Vienna, Austria, Reichert-Jung) equipped with a diamond knife (Diatome, Switzerland) at room temperature.

To study the deformation behavior of the films, we microtomed semithin sections (500 nm thick) at room temperature with the diamond knife parallel to the extrusion direction, as shown in Figure 1. The sections were stretched in a special tensile stretching device under an optical light microscopic control and were fixed in the strained state. Afterward, the deformed sections were transferred to the transmission electron microscopy (TEM) specimen holder and directly studied with an intermediate-voltage TEM instrument (JEM 4000FX, JEOL, Tokyo, Japan) operated at an accelerating voltage of 400 kV. Those studies were carried out at the Max Planck Institute for Microstructure Physics in Halle (Saale), Germany.

Mechanical testing

For measurement of the stress–strain diagrams, tensile tests were performed with a universal tensile machine (Zwick 1425, Ulm, Germany) according to DIN EN ISO 527. Miniaturized tensile test specimens (starting gauge length = 50 mm) were punched out of the extruded films with their long axis along the extrusion direction. The experiments were made at room temperature with a crosshead speed of 50 mm/min (which means that the strain rate was 100%/min) to measure the traversal displacement of the crossheads.

Rheo-optical investigations

To investigate the response of the molecules in the polymer layers during uniaxial elongation, the deformation behavior was examined with rheo-optical Fourier transform infrared (FTIR) spectroscopy.

The rheo-optical FTIR spectroscopy was performed on a Bruker IFS 88 FTIR spectrometer (Bruker Optik GmbH, Ettlingen, Germany) equipped with an mercury cadmium telluride (MCT) detector. Small strips of the multilayered films were uniaxially elongated into the extrusion direction, and FTIR spectra were acquired with the radiation polarized alternately parallel and perpendicular to the tensile direction. The incoming radiation was perpendicular to the film surface and the tensile direction (Fig. 1). The spectral resolution was 4 cm^{-1}, and 10 scans were accumulated in 3 s for one spectrum. To record enough spectra for the calculation of the orientation function values during the stretching procedure, a strain rate of only 80%/min was chosen. The difference in strain rate between the mechanical testing

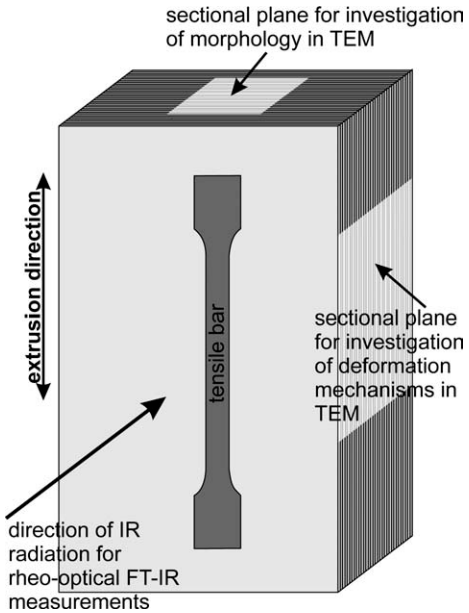

Figure 1 Scheme of the preparation of tensile test specimens for the characterization of the mechanical properties and TEM sections for the investigation of the morphology and deformation behavior. Furthermore, the measurement geometry for the rheo-optical FTIR measurement is shown.

and the rheo-optical investigations led to different forms of the stress–strain diagrams because of the known time dependence of the material behavior. The experiments were stopped at an elongation of 100, 200, or 300% of strain, depending on the macroscopic elongation at break.

RESULTS AND DISCUSSION

Characterization of the multilayer film morphologies

To characterize the multilayer construction, the morphology of the extruded films was analyzed as a function of thickness of the individual layers and the relative composition of the components. Figure 2 shows some TEM micrographs of the films. On the left side, the 90/10 PP/PS films are presented, from the thickest film to the thinnest one, and on the right side, the corresponding 70/30 PP/PS films can be seen. More micrographs and scanning electron microscopic results are illustrated in ref. [13]. To understand the contrast, one should know that the interphase between the PP and PS layers was almost black because of the staining by RuO_4, whereas the layers themselves were gray. The PS layers appeared darker than the PP phase. The areas occupied by the darker (PS) and less dark (PP) regions corresponded roughly to the PP/PS volume composition.

The inspection of the images revealed that the PP/PS films consisted of primarily continuous layers that were more or less uniform in thickness. Between these excellent layers, there were some local areas with a concentration of defects in layer construction [Fig. 2(b)]. With more irregular compositions [Fig. 2(a)] or thinner films, which implied a decrease of the thickness of the individual layers [Fig. 2(d,f)], the number of failures increased. These failures could have been ruptured layers, a combining of layers, an ending of layers, or the formation of drop-shaped ends. In addition to the already depicted defects, we found a lot of drops formed from the layer rupture of the minority phase in the thinner films. The 90/10 PP/PS film with a film thickness of only 25 μm was the extreme case of irregular composition and very thin layers. The morphology of the film was composed of small layer fragments plus domains of PS embedded in a PP matrix. In this case, the multilayered morphology of the film was almost destroyed.

Characterization of deformation during tensile loading

Later, the correlations among the observed morphology, the deformation micromechanisms, and the molecular orientation are described.

Figure 3 gives the tensile stress–strain curves of the PP/PS films as they relied on the composition and the film thickness. The films with a composition of 90/10 PP/PS were ductile. The films with a composition of 70/30 PP/PS revealed a twofold behavior. The two films with a thickness of 250 and 125 μm were brittle, whereas the thin film with a thickness of only 25 μm was ductile. For both compositions, we noticed that the elongation at break increased significantly with decreasing film thickness, that is, decreasing single-layer thickness. For the 90/10 PP/PS film with a film thickness of 25 μm, the high elongation at break could be explained through its morphology, which was more a PP filled with particle-like PS domains than a layered structure, as shown in Figure 2(e).

All of the other samples discussed in this article revealed a layered morphology. The morphology (from the composition and film thickness) and single-layer thickness had strong influences on the elongation at break. The number of defects in the layer construction affected the mechanical behavior directly. By decreasing film thickness and, therefore, the single-layer thickness, the difference between the single measurements and also the standard deviation increased. However, it should be kept in mind that the number of failures in layer construction increased with decreasing film thickness, as described previously.

For the analysis of micromechanical behavior, 500 nm thick semithin sections were investigated in a transmission electron microscope with a comparatively high voltage of 400 kV. The resulting TEM micrographs are represented in Figures 4 and 5. The strained semithin sections were not stained, but due to the composition of the multilayers, we observed that the PP appeared to be bright, and the PS appeared dark. The cavities were white. Figure 4 illustrates the micromechanics of the ductile 90/10 PP/PS films having thicknesses of 250 and 125 μm, whereas Figure 5 exhibits the deformation of the brittle 70/30 PP/PS films also having thicknesses of 250 and 125 μm. Both of the 90/10 PP/PS films had large deformation zones, and inside them, the deformation was homogeneous. Single PS particle-like domains (which were defects in layer construction) led to ruptures at the interface and stretching of the arising cavity in which the PS domains did not deform, as shown in Figure 4(b). From such cavities, a local strain of about 400% could be estimated. Besides these defects, perfectly stretched layers could be seen. The two dark PS layers above the PS domain and the surrounding cavity in Figure 4(b) got clearly thinner in the range of the cavity; this was a sign for yielding. Both the PP and PS layers were strongly dilated, reaching the same local strain as the described cavities. In Figure 4(d), the same

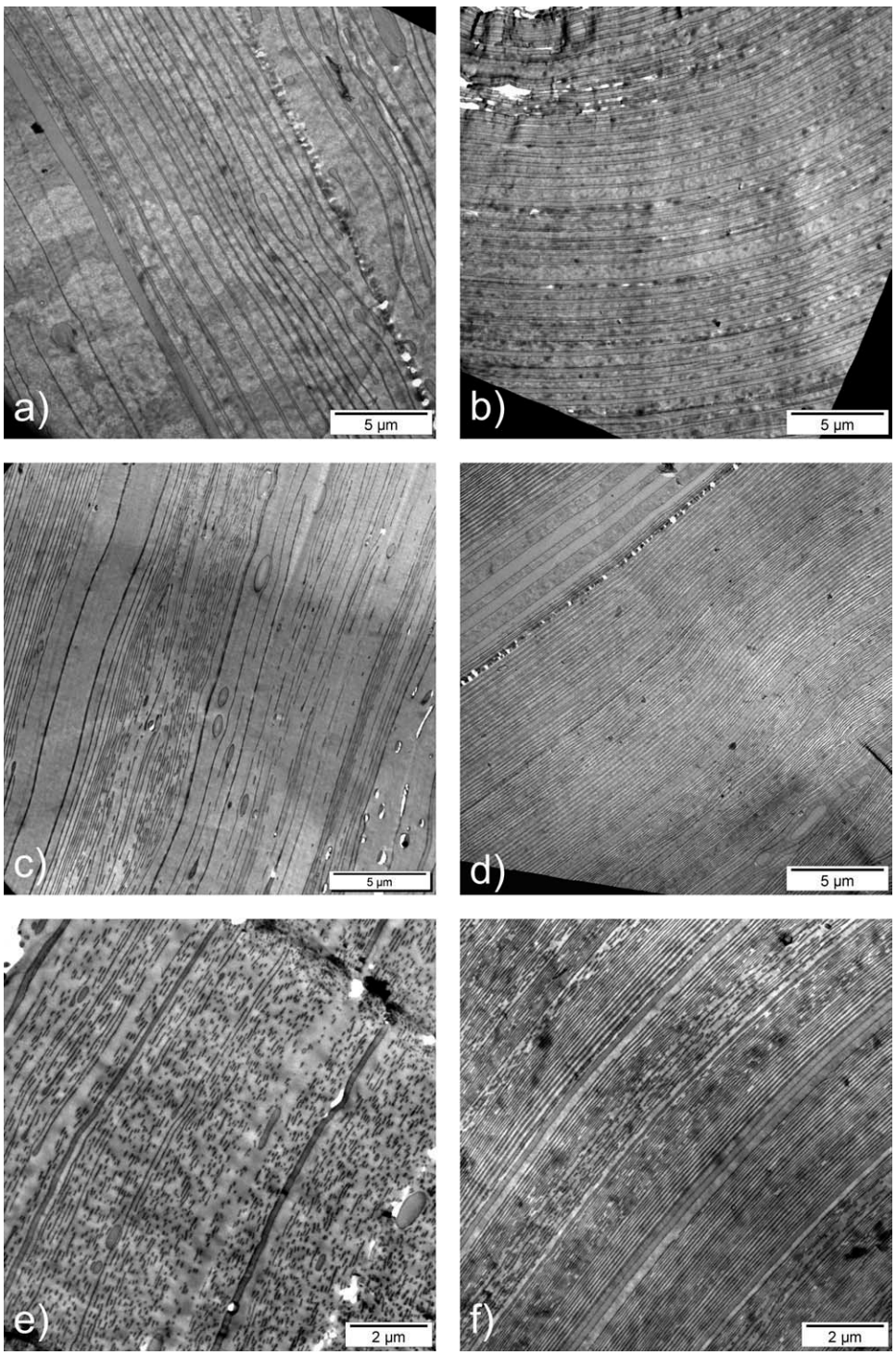

Figure 2 Morphology of the stained films shown on TEM micrographs: 90/10 PP/PS (right) and 70/30 PP/PS (left). The film thicknesses were variable: (a,b) film thickness = 250 µm, (c,d) film thickness = 125 µm, and (e,f) film thickness = 25 µm.

effects can be seen. Additionally, PS layers having thicknesses of about 280 nm and greater, which were considerably more than calculated, could be seen. These layers did not deform as homogeneously as the thin ones described previously but in local deformation zones. In these zones, delamination occurred at the interface.

In contrast to the ductile 90/10 PP/PS films, the brittle 70/30 PP/PS multilayers (Fig. 5) exhibited no large deformation areas but crazelike structures going through several PP and PS layers. The fibrils of these crazelike structures were formed by only two or three highly elongated PP and PS layers. Figure 5(d) shows another specialty of the 70/30

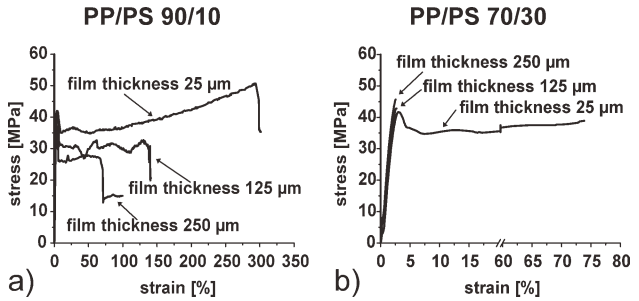

Figure 3 Tensile test curves of the PP/PS multilayered films recorded at 23°C.

PP/PS samples. There was one really thick PS layer forming typical PS crazes, which are known from the bulk. This PS layer formed one of the fibrils of the bigger crazelike structure going over several layers. Crazes in the thick PS layers cracked, as shown in Figure 5(d), destroying the layer and, therefore, the first fibril of the crazelike structure.

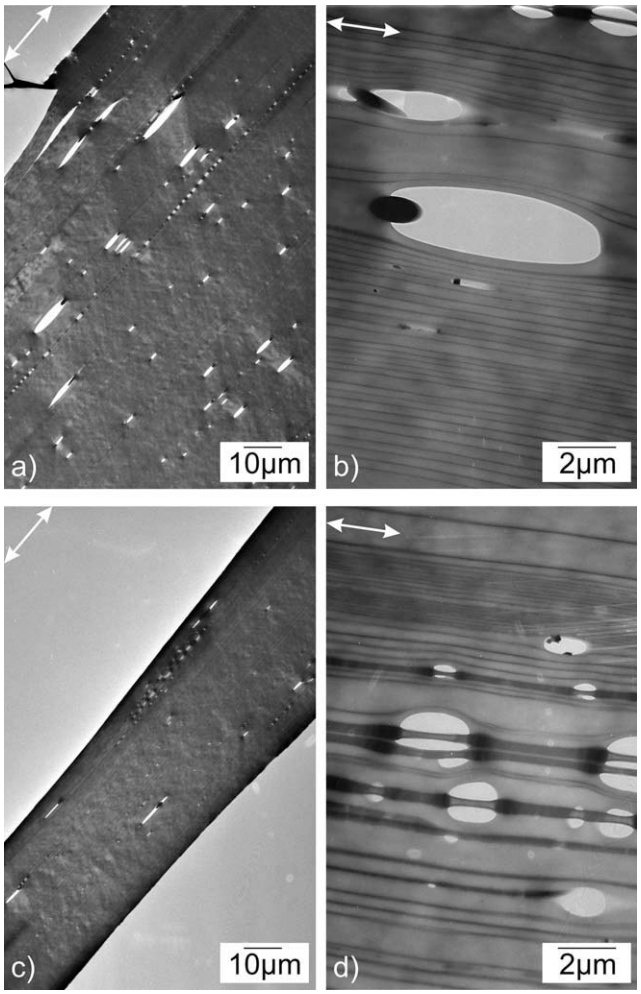

Figure 4 Overview (left) and higher magnification (right) of the deformed 90/10 PP/PS multilayers: (a,b) 250-µm film thickness and (c,d) 125-µm film thickness. The arrows on the TEM micrographs indicate the tensile direction.

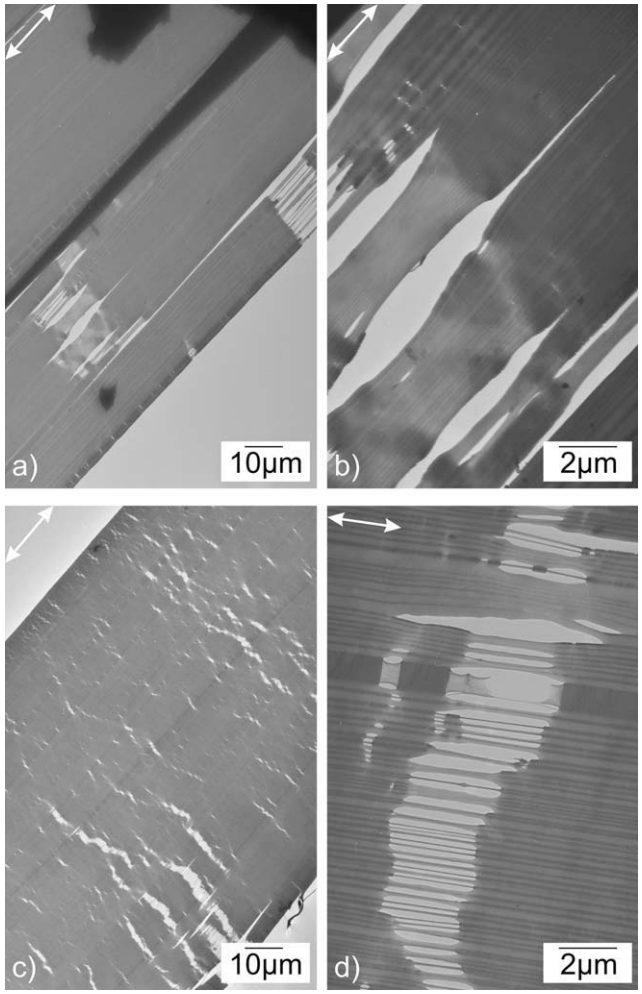

Figure 5 Overview (left) and higher magnification (right) of the deformed 70/30 PP/PS multilayers investigated by TEM: (a,b) 250-µm film thickness and (c,d) 125-µm film thickness. The arrows indicate the tensile direction.

Afterward, the next fibril of the crazelike structure broke. The rupture of fibrils continued and led to brittle behavior, which was detected by the tensile tests.

Deformation on the molecular level

The molecular behavior during deformation of the ductile 90/10 PP/PS films having layer thicknesses of 125 and 25 µm and of the 70/30 PP/PS with a film thickness of 25 µm was characterized by rheo-optical FTIR spectroscopy, as described previously. To derive information about the molecular orientation during mechanical treatment, isolated bands that were characteristic of PP and PS had to be identified. For the given system, the two bands at 1000 and 970 cm^{-1} were assigned to PP, and the band at 1600 cm^{-1} was characteristic of PS. The transition moment directions of the PP bands were parallel to the polymer chain axis, whereas the band at 1000 cm^{-1} corresponded to the crystalline (crys)

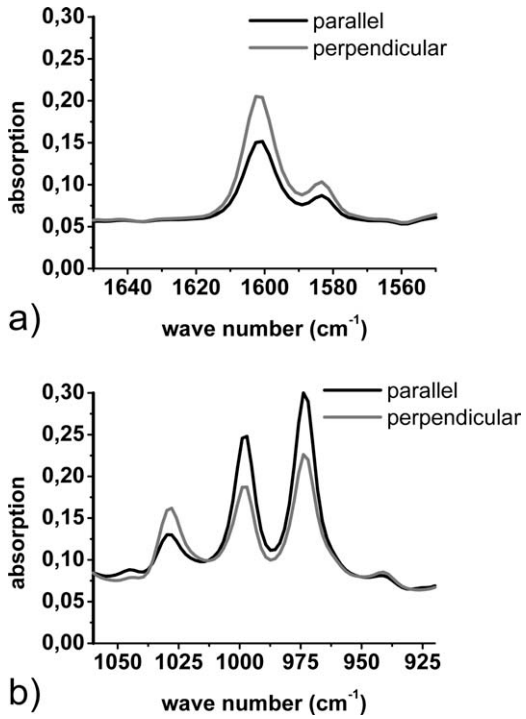

Figure 6 FTIR spectra recorded with radiation polarized parallel and perpendicular to the tensile direction of the drawn 70/30 PP/PS film with a film thickness of 25 μm: (a) PS band at 1600 cm^{-1} and (b) PP bands at 1000 and 970 cm^{-1}.

phase. Both the crystalline and amorphous (crys+am) phase contributed to the 970-cm^{-1} band. The transition moment of the PS-specific band was perpendicular to the polymer chain axis. The orientation of the polymer chains led to parallel dichroism for the PP bands and to perpendicular dichroism of the PS band (Fig. 6).

Figure 7 presents the orientation functions calculated from the dichroism[20] of the PS- and PP-specific bands as a function of strain. Both 25-μm thin films had a slight orientation in the extrusion direction (the same direction as the tensile direction) because of the film processing; this was the extrusion of a multilayered film having a thickness of about 50 μm and following stretch formation. However, for the 90/10 PP/PS 25-μm film, no orientation of PS could be measured in the beginning. This means that the stretch formation was supported by the PP phase and had no influence on PS. This fact was originated by the morphology of this sample, which was a PP matrix filled with particle-like PS domains. Compared to the orientation functions of the other films, this sample had another specialty. The orientation functions of PP, which reached values of 0.75 and 0.6, respectively, were higher than that of PS. From about 75% strain, the orientation function of PS was nearly constant. At that time, delamination at the interface of the particle-like PS domains occurred, and stretching of the arising cavities began, in a manner similar to that of the PS domain shown in Figure 4(b). Further stretching of the film just happened in the PP phase and resulted in a diminished cross section and relatively low strain at break compared to bulk PP. In contrast to that of the described film, the diagrams for the two samples having a layered morphology demonstrated that PS oriented more strongly than PP. Taking into account the theoretical maximum stretchability of about 400% for the PS,[21] we observed that the polymer chains were perfectly oriented then, and the measured strain at break of about 800% for PP,[22] with a highly fibrillated morphology with almost perfectly oriented molecules, was quite reasonable. With the same values reached for the orientation functions at break, PS must have had a sharper increase than PP.

For all three samples, independent of the phase arrangement, the orientation of crystalline PP was higher than the orientation of the average (crystalline and amorphous) PP. The same effect was observed for other semicrystalline polymers, such as polyethylene[23] and poly(ε-caprolactone).[24] This phenomenon was interpreted as follows. The molecules in the amorphous phase containing tie molecules, chain ends, branches, and coiled molecules responded very differently to tensile loading. The tie molecules could be oriented very strongly, whereas the other molecules (molecule segments) could not be oriented or could only be very slightly oriented. That means that only few molecules contributed to the deformation. In contrast, polymer chains in the crystalline lamellae were oriented uniformly. That means the lamellae and all of their molecules were rotated during tensile loading. Compared to the

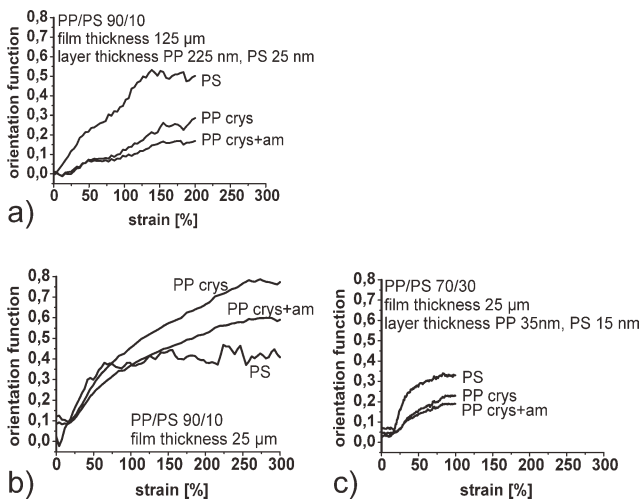

Figure 7 Orientation functions calculated from the rheo-optical FTIR measurements: (a) 90/10 PP/PS with a film thickness of 125 μm, (b) 90/10 PP/PS with a film thickness of 25 μm, and (c) 70/30 PP/PS with a film thickness of 25 μm.

orientation functions of PP in the literature,[25] similarities could be found. First, there was a small decrease (in the case of α-PP, which is presented here, it was rather constant) of orientation function. Second, there was a sharp increase followed by a smooth rise, which was the third. However, the values corresponding to the orientation functions were different from those in the literature. This could have been a consequence of the different dimensions of the samples. The investigated PP occurred in very thin layers, whereas in the literature, bulk PP was described.

CONCLUSIONS

The deformation mechanisms of multilayered PP/PS films fabricated by the layer multiplying coextrusion technique were investigated with TEM and rheo-optical FTIR measurements. To determine the macroscopic mechanical behavior, uniaxial tensile testing was performed. The findings of this work can be summarized as follows:

- The multilayered PP/PS films had primarily continuous layers that were more or less uniform in thickness. In some local areas, there were defects in layer construction. In films with a composition of 90/10 PP/PS or thin films containing thin individual layers, the number of failures increased.
- With decreasing film thickness of each composition, the elongation at break of the films was found to increase significantly. This could be correlated with a transition from brittle (film thicknesses = 250 and 125 μm) to ductile (film thickness = 25 μm) behavior for the 70/30 PP/PS films.
- The deformation of semithin sections exhibited large deformation areas for the ductile 90/10 PP/PS films (film thicknesses = 250 and 125 μm) and crazelike structures extending through several layers for the brittle 70/30 PP/PS compositions (film thicknesses = 250 and 125 μm).
- At the same strain, the orientation of PS molecules was higher than the orientation of PP in the layered morphology. The 90/10 PP/PS film with a film thickness of 25 μm, which was a PP filled with particle-like PS domains, showed a converse effect. At strains higher than 75%, the orientation of PP molecules was higher than that of the orientation of PS molecules.
- No orientation of molecules due to film-forming processes could be found for the 125 μm thick 90/10 PP/PS film. However, for both investigated 25-μm thin films, an orientation of PP molecules in the extrusion direction due to the film-forming process was detected. The processing of the 25 μm thick 70/30 PP/PS film also led to an orientation in the extrusion direction of the PS molecules.

The authors thank E. Baer and A. Hiltner from Case Western Reserve University (Cleveland, OH) for preparing and providing the films. They also thank them for the discussions, which helped them continue the work on the multilayered materials.

References

1. Bernal-Lara, T. E.; Ranade, A.; Hiltner, A.; Baer, E. In Mechanical Properties of Polymers Based on Nanostructure and Morphology; Michler, G. H., Baltá-Calleja, F. J., Eds.; Taylor & Francis: Boca Raton, FL, 2005; Chapter 15.
2. Pethe, V. V.; Wang, H. P.; Hiltner, A.; Baer, E.; Freeman, B. D. J Appl Polym Sci 2008, 110, 1411.
3. Mueller, C.; Topolkaraev, V.; Soerens, D.; Hiltner, A.; Baer, E. J Appl Polym Sci 2000, 78, 816.
4. Jin, Y.; Tai, H.; Hiltner, A.; Baer, E.; Shirk, J. S. J Appl Polym Sci 2007, 103, 1834.
5. Nazarenko, S.; Hiltner, A.; Baer, E. J Mater Sci 1999, 34, 1461.
6. Mueller, C.; Kerns, J.; Ebeling, T.; Nazarenko, S.; Hiltner, A.; Baer, E. Polym Process Eng 1997, 97, 137.
7. Ma, M.; Vijayan, K.; Im, J.; Hiltner, A.; Baer, E. J Mater Sci 1990, 25, 2039.
8. Haderski, D.; Sung, K.; Im, J.; Hiltner, A.; Baer, E. J Appl Polym Sci 1994, 52, 121.
9. Sung, K.; Haderski, D.; Hiltner, A.; Baer, E. J Appl Polym Sci 1994, 52, 147.
10. Kerns, J.; Hsieh, A.; Hiltner, A.; Baer, E. J Appl Polym Sci 2000, 77, 1545.
11. Kerns, J.; Hsieh, A.; Hiltner, A.; Baer, E. Macromol Symp 1999, 147, 15.
12. Ivan'kova, E. M.; Krumova, M.; Michler, G. H.; Koets, P. P. Colloid Polym Sci 2004, 282, 203.
13. Scholtyssek, S.; Adhikari, R.; Seydewitz, V.; Michler, G. H.; Baer, E.; Hiltner, A. Macromol Symp 2010, 294, 33.
14. Jin, Y.; Rogunova, M.; Hiltner, A.; Baer, E.; Nowacki, R.; Galeski, A.; Piorkowska, E. J Polym Sci Part B: Polym Phys 2004, 42, 3380.
15. Bernal-Lara, T. E.; Masirek, R.; Hiltner, A.; Baer, E.; Piorkowska, E.; Galeski, A. J Appl Polym Sci 2006, 99, 597.
16. Pan, S. J.; Im, J.; Hill, M. J.; Keller, A.; Hiltner, A.; Baer, E. J Polym Sci Part B: Polym Phys 1990, 28, 1105.
17. Jin, Y.; Hiltner, A.; Baer, E.; Piorkowska, E.; Galeski, A. J Polym Sci Part B: Polym Phys 2006, 44, 1795.
18. Ania, F.; Baltá-Calleja, F.J.; Flores, A.; Michler, G.H.; Scholtyssek, S.; Khariwala, D.; Hiltner, A.; Baer, E.; Rong, L.; Hsiao, B.S. Eur Polym J 2012, 48, 86.
19. Adhikari, R.; Seydewitz, V.; Löschner, K.; Michler, G. H.; Hiltner, A.; Baer, E. Macromol Symp 2010, 290, 156.
20. Hoffmann, U.; Pfeifer, F.; Okretic, S.; Völkl, N.; Zahedi, M.; Siesler, H. W. Appl Spectrosc 1993, 47, 1531.
21. Michler, G.H. Kunststoffmikromechanik - Morphologie, Deformations- und Bruchmechanismen; Hanser: Munich, 1992.
22. Oberbach, K. Kunststofftaschenbuch, 28. Ausgabe; Hanser: Munich, 2001.
23. Glenz, W.; Peterlin, A. J Polym Sci Part A-2: Polym Phys 1971, 9, 1191.
24. Keroack, D.; Zhao, Y.; Prud'homme, R. E. Polymer 1998, 40, 243.
25. Huy, T. A.; Adhikari, R.; Lüpke, T.; Henning, S.; Michler, G. H. J Polym Sci Part B: Polym Phys 2004, 42, 4478.